SPE
Society of Petroleum Engineers

SPE 16009

Application of a Multiple Porosity/Permeability Simulator in Fractured Reservoir Simulation

by B.Y.Q. Lee and T.B.S. Tan, D&S Petroleum Consulting Group Ltd.

SPE Members

This paper was prepared for presentation at the Ninth SPE Symposium on Reservoir Simulation held in San Antonio, Texas, February 1-4, 1987

Abstract

This paper presents the modelling of naturally fractured reservoirs using a multi-porosity multi-permeability thermal simulator. An iterative solution technique that allows connection between any pair of blocks is used.

Dual-porosity and triple-porosity systems are simulated. Results follow those of the analytical methods. Simulation of a thermal recovery scheme using a horizontal steam injector and a horizontal producer in a naturally fractured heavy oil reservoir is presented as an example.

Introduction

Naturally fractured reservoirs have been studied extensively over the last decades. The behaviour of naturally fractured reservoirs was simulated by Kazemi.[12] Since then, tremendous progress was made by other authors.[13-15,18]. Although numerical simulation of naturally fractured reservoir had been reported by many authors[12-18], majority of the research was done on analytical methods. Warren and Root[1] proposed the idealization of using two domains, one for the fracture and the other for the matrix, to describe the heterogeneity for well test analysis. The fracture domain has a low storativity and high permeability whereas the matrix domain is the exact opposite. It is assumed that fluid will flow to the well only through the fracture domain. This idealization is often called dual-porosity. Figure 1 shows an idealized dual-porosity model.

Warren and Root[1] assumed a quasi-steady state interporosity flow between the fracture and matrix. Later on, other authors[2-8] suggested the use of transient interporosity flow models. Upon solving the equations analytically, a transient interporosity flow model gives a steeper transition curve on a semi-log plot. Some authors[3-8] show that the curve is actually a straight line and its value is related to other parameters such as the fracture storativity (ω).

From the simulation point of view, the transient behavior could be simulated by better definition of the matrix domain. Figure 2 shows a matrix being subdivided into different grid cells. With a finer grid system, the transient effect could be simulated more readily. A coarser grid would give a behavior closer to that of the pseudo-steady state interporosity flow.

Recently, triple-porosity was proposed by some authors[9-11]. It assumes that there are two matrix domains and one fracture domain. The two matrix domains are different in properties and don't flow to each other. Figure 3 is an idealized triple-porosity model. In the absence of wellbore storage, the pressure transient behavior of dual-porosity system shows two parallel straight lines on a semi-log plot. It is possible for a triple-porosity system to show three parallel straight lines if one of the matrix domains has the lower storativity and higher interporosity flow coefficient. Otherwise, the behavior will be just like that of the dual-porosity and only two parallel straight lines will appear.

The simulator used in this paper allows connections between any two blocks in the grid system and an iterative solution was used to solve the resultant matrix. This flexibility makes the triple-porosity configuration and subdivision of the matrix domain very straight forward.

References and illustrations at end of paper.

The modelling of a dual-porosity dual-permeability heavy oil reservoir with a horizontal steam injector and producer is also investigated. In addition to the interporosity flow coefficient, a parameter called interporosity heat transfer coefficient is needed in order to model the heat flow properly.

Mathematical Formulation

The simulation model is a fully implicit, three-dimensional, multiphase, multicomponent thermal model capable of simulating steam and combustion recovery processes. In addition to five- and nine-point finite difference approximation, the model allows the linking of any pair of grid cells for the transfer of mass and energy. It is this particular feature that allows the simulation of dual-porosity, dual-permeability systems, triple-porosity/permeability systems and all the way to multiple porosity/permeabilty systems.

The formulation for dual-porosity/permeability systems is presented so that the logical extension to multiple porosity/permeability systems can be easily made.

In dual-porosity/permeability systems, the reservoir grid is divided into two partitions, one of which will have the porosity and permeability of the fracture, and the other, the properties of the matrix. Each cell in the matrix domain is linked to the corresponding cell in the fracture domain by interporosity transfer coefficients for mass and energy.

Any component can exist in any phase and we assume there are N phases, Nc components, Nrx reactions. For any cell in either domain, the conservation equations are identical.

Component Balance, i = 1,Nc

$$\sum_{n=1}^{N} \Delta \left[T \frac{k_{rn}}{\mu_n} \rho_n x_{in} (\Delta P + \Delta P_{cn} - \gamma_n \Delta z)\right]$$

$$+ \sum_{n=1}^{N} T_{maf} \frac{k_{rn}}{\mu_n} \rho_n x_{in} (\Delta P_{maf} + \Delta P_{cnmaf} - \gamma_n \Delta z_{maf})$$

$$= \frac{V}{\Delta t} \delta \left(\phi \sum_{n=1}^{N} \rho_n S_n x_{in}\right) + \sum_{rx=1}^{Nrx} q_{irx} + q_i \quad \text{.....1}$$

$$\text{and } \Delta P_{maf} = P_{ma} - P_f \text{ or } P_f - P_{ma} \quad \text{.....2}$$

The matrix-fracture interporosity transmissibility T_{maf} is defined as:

$$T_{maf} = (Vk\sigma)_{ma} \quad \text{.....3}$$

The interporosity transmissibility is an important parameter since it controls the communication between two different domains. In order to evaluate it, σ will have to be known. Unfortunately, σ is a very difficult parameter to evaluate because it is a shape factor which depends on matrix block size. Thomas[13] outlined three methods of calculating σ.

$$\sigma = \frac{4N_f(N_f+2)}{L^2} \quad \text{.....4A}$$

$$\sigma = \frac{A}{LV} \quad \text{.....4B}$$

$$\sigma = 4\left(\frac{1}{L_x^2} + \frac{1}{L_y^2} + \frac{1}{L_z^2}\right) \quad \text{.....4C}$$

Equation 4A was originally proposed by Warren and Roots[1]. N_f is the number of normal sets of fractures. Equation 4C was originally proposed by Kazemi[12]. L_x, L_y, and L_z are the lengths of the matrix block. The above equations do not yield the same σ. Naturally, other equations could be used depending how one perceives the geometry. Practically speaking, σ is just a matching parameter and can be estimated by history matching a well test.

Energy Balance

$$\sum_{n=1}^{N} \Delta \left[T \frac{k_{rn}}{\mu_n} \rho_n H_n (\Delta P + \Delta P_{cn} - \gamma_n \Delta z)\right] + \Delta(T_c \Delta T)$$

$$+ \sum_{n=1}^{N} T_{maf} \frac{k_{rn}}{\mu_n} \rho_n H_n (\Delta P_{maf} + \Delta P_{cnmaf} - \gamma_n \Delta z_{maf})$$

$$+ T_{cmaf} (\Delta T_{maf})$$

$$= \frac{V}{\Delta t} \delta\left[\left(\phi \sum_{n=1}^{N} \rho_n S_n U_n\right) + (1-\phi)(\rho c_p)_R (T - T_b)\right]$$

$$+ \sum_{rx=1}^{N_{rx}} H_{rx} + q_H + q_{o/u} \quad \text{.....5}$$

The matrix-fracture interporosity heat transfer coefficient is defined as:

$$T_{cmaf} = (VK\sigma)_{ma} \quad \text{.....6}$$

where K is thermal conductivity, σ is defined as in equation 4, and

$$\Delta T_{maf} = T_{ma} - T_f \text{ or } T_f - T_{ma} \quad \ldots\ldots\ldots 7$$

Typically T_{cmaf}, like T_{maf}, is defined by the user and used as matching parameters.

The usual saturation constraint and mole fraction constraint, reaction rate equations complete the mathematical formulation. If required, implicit bottom hole pressures and well constraints will also be incorporated into the final Jacobian.

For triple-porosity systems, three partitions in a grid system will be set up and links established between the fracture domain and the two matrix domains. Furthermore, the user can define permeability in one of the matrix domains (triple-porosity, dual-permeability) or in all domains (triple-porosity and triple-permeability). Locally within each domain the porosity and permeability can also be modified, as well as individual interporosity mass transfer and heat transfer coefficients. The number of possible combinations are limitless. A matrix domain can be further partitioned into two or more domains and linked to each other as well as to the fracture domain for finer definition of imbibition, drainage and heat transfer mechanisms.

The mass balance and energy balance equations (equations 1 and 5) are written for a dual-porosity system. Without the interporosity transfer terms, the equations will be identical to a "single porosity" formulation which is also used in this model for flow within the same domain. For each additional domain, an extra interporosity transfer term will be needed for each equation.

Iterative Matrix Solution

As a result of the non-neighbour connections used to connect grid cells in the matrix domain(s) with the cells in the fracture domain, the Jacobian coefficient matrix loses the regular banded structure associated with normal five-point or nine-point difference schemes. Figure 7 shows the incidence matrix corresponding to the grid cell system of Figure 5.

The iterative solution method used in the thermal model can solve any matrix structure resulting from connecting any cell to any other cell. The basis of the method is an incomplete LU factorization. In direct solution, when the LU factorization is carried out, matrix fill-in occurs along rows in the L matrix from the off diagonal terms to the main diagonal, and along columns in the U matrix. When some of the induced terms are omitted in the fill-in process, an iterative method results. The convergence of the iterative method will depend on the appropriate selection of the induced terms. Poor selection will lead to divergence. A previous paper[19] discusses the selection of induced terms for an alternate diagonal ordering. The current implementation is completely general.

The criterion for selection is the relative magnitude of the induced terms rather than their position. Thus symbolic factorization which places induced terms on a first, second, or third degree basis is not used. Since the off diagonal terms in the coefficient matrix have a common factor, that is the transmissibility coefficients, a matrix consisting only of these is first set up. This is factorized and the induced terms are sorted out in descending order of magnitude. Selection of induced terms then proceeds. The number of induced terms for each grid cell, so called the computational molecule, would depend on the number of connections, the magnitude of the induced terms and the storage space available. Thus each grid cell will have a completely difference computational molecule based on the orientation of the transmissibilities of the neighbouring cells. No convergence difficulties for highly anisotropic problems have ever been encountered, unlike other methods which sweep in fixed co-ordinate directions.

Furthermore, as the simulation proceeds and the transmissibilities vary as various mobility fronts pass through the grid system, the selection process for induced terms as described above is repeated. Thus the computational molecule for each grid block is also dynamic and adapts itself to changing reservoir behaviour.

Following the incomplete factorization, the normal forward and backward substitution is performed. Due to the general nature of the algorithm, implicit bottomhole pressures for wells together with constraint equations can be easily incorporated.

Sample Case I - Dual-Porosity

Dual-porosity idealization has been widely used in well test analysis of naturally fractured reservoirs. One of the characteristics of the model is the presence of two parallel straight lines on a semi-log plot such as MDH plot or Horner plot. A single phase radial model was set up to demonstrate the viability of using a simulator to model dual-porosity behavior. Figure 4 is a schematic diagram of a grid system for simulation. Table 1 shows the data being used for the model. The drawdown behavior was simulated. Figure 8 is an MDH plot of the pressure response. Two parallel straight lines and a transition curve were obtained. Using equation 8, the ω can be calculated.

$$\omega = \frac{(\phi C_t)_f}{(\phi C_t)_f + (\phi C_t)_{ma}} = 10^{\frac{-\Delta P}{m}} \quad \ldots\ldots\ldots 8$$

From the slope and vertical displacement of the two straight lines, ω and kh were calculated as 0.1 and 5013 which were in excellent agreement with the theoretical values.

When Warren and Root[1] first solved the dual-porosity equations, quasi-steady state flow between the fracture and matrix was assumed. Later on, transient interporosity flow was proposed by many authors[2-8]. The major difference between the two assumptions is in the transition period. Pseudo-steady state interporosity flow gives a flatter response while the transient interporosity flow gives a much steeper curve. As a matter of fact, many authors have proved that a straight line actually exists. For example, Gringarten[3] et al showed that the transition slope should be 1/2 of the final slope. Cinco-Ley[4] et al and other authors[6-7] determined that the slope is related to other parameters such as ω and should have a minimum value of half of the final slope.

When using a simulator such as the one used in this paper, the transient interporosity flow can be simulated by better definition of the matrix domain. Figure 5 is a schematic diagram of using more than one grid cell for the matrix domain. Obviously the σ for the matrix cell that is connected to the fracture cell will have to be re-calculated. The calculation of σ would be a confusing issue as there are quite a few ways to subdivide the matrix. Figure 2 shows three ways the matrix could be subdivided. Practically speaking, the σ will just be a matching parameter.

In order to simulate the transient interporosity flow, the matrix domain is subdivided into two and four cells. Results of the two cases and the single cell case are shown on Figure 9. The rather flat response on the single cell case resembles the quasi-steady state flow proposed by Warren and Root[1], whereas the other two cases give a steeper curve and an earlier start of the transition period. Using a simulator with a different approach in formulation and solution technique, Gilman[18] arrived at the same conclusion.

Sample Case 2 - Triple-Porosity

It appears that the first triple-porosity paper was presented by Liu[9]. Abdassah[10] et al published their work on the formulation and use of triple-porosity in well test analysis of naturally fractured reservoir. Cinco-Ley[11] et al had also reported the pressure transient behavior of multiple porosity systems. Simulation using triple-porosity idealization was also reported by Leung[16]. Pruess[14] et al reported some sample cases using a simulator similar to the one used in this paper; although a triple-porosity case was not investigated. In a triple-porosity system, two domains are used to describe the matrix. Fluid will flow to the well through the fractures only. Figure 3 is an idealized model of a triple-porosity system. Figure 6 is a schematic diagram of a grid system for simulation.

The behavior of triple-porosity could be viewed as an extension to the dual-porosity. Certain conclusions such as presence of parallel straight lines on semi-log plot are similar. It is possible to have three parallel straight lines if $\omega_1 > \omega_2$ and $\lambda_1 > \lambda_2$. ω_1 and ω_2 are defined as follows:

$$\omega_1 = \frac{(\phi C_t)_f}{(\phi C_t)_{ma1} + (\phi C_t)_f} \quad \text{.....9}$$

$$\omega_2 = \frac{(\phi C_t)_f}{(\phi C_t)_{ma2} + (\phi C_t)_f} \quad \text{.....10}$$

λ is the interporosity flow parameter used in analytical method. In the case when $\omega_1 > \omega_2$ and $\lambda_1 < \lambda_2$, only two parallel straight lines will appear and the response is just like the behavior of a dual-porosity system.

A single phase radial model was constructed to simulate the drawdown of a triple-porosity system. Table 2 shows the parameters used in the model. Figure 10 shows the cases when $\lambda_1 > \lambda_2$ and λ_2 is held constant in each case. Three parallel straight lines can be drawn on the MDH plot. The second parallel straight line becomes shorter as λ_1 approaches λ_2. It finally disappears when λ_1 equals to λ_2. In this case, the triple-porosity system is reduced to a dual-porosity one. Figure 11 shows the cases when $\lambda_1 < \lambda_2$. As mentioned previously, only two parallel straight lines appear.

When $\omega_1 > \omega_2$ and $\lambda_1 > \lambda_2$, the storativity of matrix 1 is smaller and its transmissibility is higher. Its response will overshadow that of matrix 2 in the earlier time. As time increases, matrix 1 will be depleted to the point that the flow from matrix 2 becomes the dorminant response. When $\omega_1 > \omega_2$ and $\lambda_1 < \lambda_2$, both the storativity and transmissibility of matrix 1 are lower. The matrix 2 will therefore respond earlier and, because of its higher storativity, will stay dorminant throughout. As a result, only two parallel straight lines will appear. Although three parallel straight lines are possible in a triple-porosity system, they could only be seen when the ω's and λ's are very different. In practice, it is very difficult to see even just two parallel straight lines because of factors such as wellbore storage. Abdassah[10] et al and Cinco-Ley[11] et al suggested using the derivative approach in analyzing the triple-porosity system.

The parallel straight lines are related to each other. When three parallel straight lines are present, the relationship between the first two is:

$$\frac{(\phi C_t)_f}{(\phi C_t)_{ma1} + (\phi C_t)_f} = 10^{\frac{-\Delta P_1}{m}} \quad \text{.....11}$$

Where ΔP_1 is the vertical displacement between the first and second straight lines. The relationship between the first and third parallel straight lines is:

$$\frac{(\phi C_t)_f}{(\phi C_t)_{ma1} + (\phi C_t)_{ma2} + (\phi C_t)_f} = 10^{\frac{-\Delta P}{m}} \quad ...12$$

Where Δp is the vertical displacement between the two straight lines. Combining equations 11 and 12, the relationship between second and third parallel straight lines is:

$$\frac{(\phi C_t)_{ma1} + (\phi C_t)_f}{(\phi C_t)_{ma1} + (\phi C_t)_{ma2} + (\phi C_t)_f} = 10^{\frac{-\Delta P_2}{m}} \quad ...13$$

Where ΔP_2 is the vertical displacement between the two straight lines.

When only two parallel straight lines are present, the relationship of equation 12 is to be used.

Sample Case 3 - Dual-Porosity/Permeability Heavy Oil Reservoir

The recovery mechanisms for a steam-assisted gravity drainage[21] of a dual-porosity, dual-permeability heavy oil reservoir are simulated. The example is not intended to be representative of any actual field or operating practice. The fluid properties of the crude oil are taken from the Fourth SPE Comparative Solution project for steam modelling[20]. The crude oil is characterized by one heavy component and all physical properties are identical to those in the reference paper, except for the oil density which is increased to 64.5 lbs/cu.ft. so that it is heavier than water.

The grid system used is a 10 cell by 10 cell vertical cross-section grid. Columns 1-5 are used to model the matrix domain and columns 6-10 are used for the fracture domain. Table 3 details the reservoir description. The physical dimensions of the two domains are identical. Fluid and thermal transmissibilities between columns 5 and 6 are zeroed out since they belong in different domains. However, special connections are established between each cell in the matrix domain and the corresponding cell in the fracture domain. Interporosity flow coefficients and heat transfer coefficients are calculated using a σ of 3. No heat losses are allowed from the fracture domain. An injection well is placed at column 1 and layer 9 in the matrix and in the corresponding fracture cell at column 6 and layer 9. A production well is placed at column 1 and layer 10 and at column 6 and layer 10. Thus this is half of a symmetrical vertical cross-section through the horizontal well.

The porosity of the fracture domain is 0.02 and the porosity of the matrix domain is 0.28. Thus the fracture blocks have much smaller pore volume. The permeability in the fracture domain is 2000 md while that of the matrix is 50 md. Heat and mass transfer is allowed in each domain. This is, therefore, a dual-porosity, dual permeability reservoir.

The saturation curves in the matrix domain are the same as those in the reference[20]. However, straight line relative permeability curves are used in the fracture domain as in Table 4. The simulator is initialized in the matrix domain with a water saturation of 45 percent and in the fracture domain with a water saturation of 95 percent. Steam is injected at an injection pressure of 155 psi and the flowing bottom hole pressure of the producing well is set at 154 psi. The model was run to 730 days.

Figure 12 shows the growth of the steam chambers in the fracture domain and the matrix domain. The percent recovery of oil versus time is shown in Figure 13. The production statistics reported by the model indicate that 91 percent of the oil was produced by the fracture interval of the producing well. The initial oil in place in the fracture domain was only 0.65 percent of the total oil in place. This shows that the oil was pushed from the matrix domain to the fracture domain via the interporosity transfer coefficients as a result of thermal expansion and steam drive. The much higher mobility of the fracture domain allowed the hot oil to drain rapidly down the fracture to the producing well.

Without the fracture domain, it is very likely that viscosity blocking would have occurred as the hot oil would be pushing against viscous cold oil raising the pressure and reducing the steam injection rate. The steam chamber grows much more rapidly in the fracture zone because of the much smaller pore volumes and the initial high water saturation. Saturation changes as much as 70 percent over a single timestep were reported by the simulator. The run took 2 hours and 7 minutes on a VAX11/780, 241 timesteps and 1680 Newton iterations for a simulation period of 730 days.

Conclusions

From the results of this work, the following comments are pertinent:

1. A simulator allowing flow between non-adjacent blocks has been developed. It is a viable tool for modelling naturally fractured reservoirs.

2. A dual-porosity system was modelled by the subject simulator. As predicted by analytical methods, two parallel straight lines were obtained on a semi-log plot. With more grid cells to represent the matrix domain, the transient response will resemble that of transient interporosity flow.

3. A triple-porosity system was simulated. When one of the matrix domains has the lower storativity and higher transmissibility, three parallel straight lines will appear on the semi-log plot. If both storativity and transmissibility of one domain are lower, then only two parallel straight lines can be obtained.

4. Simulation of a dual-porosity dual-permeability heavy oil reservoir with horizontal injector and producer was performed. Results show that the majority of produced oil, in this case 91 percent, was recovered through the fractured domain. Both the interporosity flow coefficient and heat transfer coefficient are vital to the recovery.

Nomenclature

A	Surface area for interporosity flow (ft^2)
$(\rho c_p)_R$	Heat capacity of reservoir rock (Btu/ft^3-°F)
C_t	Total compressibility (psi^{-1})
H	Enthalpy (Btu/lb mole)
K	Thermal conductivity (Btu/ft-day-°F)
k	Permeability (md)
k_r	Relative permeability
kh	Flow capacity (md-ft)
m	Slope on MDH/Horner plot (psi/cycle)
p	Pressure (psi)
p_c	Capillary pressure (psi)
Δp	Vertical displacement between two parallel straight lines on semi-log plot (psi)
q_i	Flowrate of component i (md/day)
$q_{o/u}$	Heat loss to over/under burden (Btu/day)
q_H	Heat flowrate (Btu/day)
s	Saturation
T	Temperature (°F)
U	Internal energy of phase (Btu/lb mole)
V	Bulk Volume (ft^3)
x_{in}	Mole fraction of component i, in phase n
z	Subsea depth (feet)

Greek

β	Formation volume factor
γ	Fluid gradient (psi/ft)
ϕ	Porosity
ρ	Density (lb mole/ft^3)
λ	Interporosity flow parameter
σ	Geometric parameter ($1/ft^2$)
T	Physical transimissibility (ft^3-cp/day-psi)
T_c	Heat transmissibility (Btu/day-°F)
μ	Viscosity (cp)
ω	Storativity ratio

Subscript

i	Component
n	Phase
ma	Matrix in dual-porosity system
ma1	First matrix in triple-porosity system
1	First matrix in triple-porosity system
ma2	Second matrix in triple-porosity system
2	Second matrix in triple-porosity system
rx	Reaction

References

1. Warren, J. E. and Root, P. J.: "The Behavior of Naturally Fractured Reservoirs", SPEJ (Sep, 1963) 245-255; Trans. AIME, Vol. 228.

2. deSwaan, A. O.: "Analytical Solutions for Determining Naturally Fractured Reservoir Properties by Well Testing", SPEJ (Jun,1976) 117-122.

3. Bourdet, D. and Gringarten, A. C.: "Determination of Fissure Volume and Block Size in Fractured Reservoirs by Type-Curve Analysis", paper SPE 9293, presented at the 55th Annual Fall Technical Conference and Exhibition of the SPE-AIME, Dallas, Sep. 21- 24, 1980.

4. Cinco-Ley, H. and Samaniego, F. V.: "Pressure Transient Analysis for Naturally Fractured Reservoirs", paper SPE 11026, presented at the 57th Annual Fall Technical Conference and Exhibition of the SPE-AIME, New Orleans, Sep. 26-29, 1982.

5. Streltsova, T. D.: "Well Pressure Behavior of a Naturally Fractured Reservoir", paper SPE 10782, presented at the 1982 California Regional Meeting of the SPE-AIME, San Francisco, Mar 24-26, 1982.

6. Lai, C. H., Bodvarsson, G. S., Tsang, C. F. and Witherspoon, P. A.: "A New Model for Well Test Data Analysis for Naturally Fractured Reservoirs", paper SPE 11688, presented at the 1983 California Regional Meeting of SPE-AIME, Venturea, Mar. 23-25, 1983.

7. Ohaeri, C. U.: "Pressure Buildup Analysis for a Well Produced at a Constant Pressure in a Naturally Fractured Reservoir", paper SPE 12009, presented at the 58th Annual Technical Conference and Exhibition of the SPE-AIME, San Francisco, Oct. 5-8, 1983.

8. Serra, K., Reynolds, A. C. and Raghavan, R.: "New Pressure Transient Analysis Methods for Naturally Fractured Reservoirs", JPT (Dec, 1983) 2271-2283.

9. Liu, C.: "The Unsteady Radial Flow of Compressible Liquids Through a Medium With Multiple Porosity", paper SPE 10580, presented at the SPE-AIME International Meeting on Petroleum Engineering, Beijing, China, Mar. 19-22, 1982.

10. Abdassah, D. and Ershaghi, I.: "Triple-Porosity Systems for Representing Naturally Fractured Reservoirs", SPE Formation Evaluation (Apr, 1986) 113-127.

11. Cinco-Ley, H. and Samaniego, F. V.: "The Pressure Transient Behavior for Naturally Fractured Reservoirs With Multiple Block Size", paper SPE 14168, presented at the 60th Annual Technical Conference and Exhibition of the SPE-AIME, Las Vegas, Sep. 22-25, 1985.

12. Kazemi, H.: "Pressure Transient Analysis of Naturally Fractured Reservoirs with Uniform Fracture Distribution", SPEJ (Dec, 1969) 451-462.

13. Thomas, L. K., Dixon, T. N., and Pierson, R. G.: "Fractured Reservoir Simulation", SPEJ (Feb, 1983) 42-54.

14. Pruess, K., and Narasimhan, T. N.: "A Practical Method for Modelling Fluid and Heat Flow in Fractured Porous Media", paper SPE 10509, Presented at the 6th SPE Symposium on Reservoir Simulation, New Orleans, Jan. 31 - Feb. 3, 1982.

15. Gilman, J. R., and Kazemi, H.: "Improvements in Simulation of Naturally Fractured Reservoirs", paper SPE 10511, Presented at the 6th SPE Symposium on Reservoir Simulation, New Orleans, Jan. 31 - Feb. 3, 1982.

16. Leung, W. F.: "A General Purpose Single-Phase Naturally Fractured (Carbonate) Reservoir Simulator With Rigorous Treatment of Rock-Stress/Fluid Pressure Interactions and Interporosity Flow", paper SPE 13528, Presented at the SPE 1985 Reservoir Simulation Symposium, Dallas, Feb. 10-13, 1985.

17. Wu, Y. S. and Pruess, K.: "A Multiple-Porosity Method for Simulation of Naturally Fractured Petroleum Reservoirs", paper SPE 15129, Presented at the 56th California Regional Meeting of the SPE-AIME, Oakland, Apr. 2-4,1 1986.

18. Gilman, J. R.: "An Efficient Finite- Difference Method for Simulating Phase Segregation in the Matrix Blocks in Double-Porosity Reservoirs", paper SPE 12271, Presented at the SPE 1983 Reservoir Simulation Symposium, San Francisco, Nov. 15-18, 1985; SPE Reservoir Engineering (July 1986) 403-413.

19. Tan, T. B. S., and Letkeman, J. P.: "Application of D4 Ordering and Minimization in an Effective Partial Matrix Inverse Iterative Method", paper SPE 10493, presented at the 6th SPE Symposium on Reservoir Simulation, New Orleans, Jan. 31 - Feb. 3, 1982.

20. Aziz, K., Ramesh, B., and Woo, P. T.: "Fourth SPE Comparative Solution Project: A Comparison of Steam Injection Simulators", paper SPE 13510 presented at the 8th SPE Symposium on Reservoir Simulation, Dallas, Texas, Feb. 10-13, 1985.

21. Butler, R. M.: "A New Approach to the Modelling of Steam-Assisted Gravity Drainage", J. Cdn. Pet. Tech, (May-June, 1985) 42-51.

TABLE 1

DATA FOR SAMPLE CASE 1 - DUAL-POROSITY

P_i	= 2500 psi
β	= 1.0
μ	= 0.8cp
ρ	= 62.4 lb/ft^3
C_f	= C_{ma} = 3 x 10^{-6} psi^{-1}
k_f	= 100 md
k_{ma}	= 1 md
ϕ_f	= 0.02
ϕ_{ma}	= 0.18
h	= 50 ft.
σ	= 4.94 10^{-4} ft^{-2}
Outer radius	= 6000 ft.
r_w	= 0.25 ft.
Flowrate	= 50 Stb/day

TABLE 2

DATA FOR SAMPLE CASE 2 - TRIPLE-POROSITY

P_i	= 2500 psi
β	= 1.0
μ	= 0.8 cp
ρ	= 62.4 lb/ft^3
C_f	= C_{ma1} = C_{ma2} = 3x10^{-6} psi^{-1}
k_f	= 200 md
k_{ma1}	= k_{ma2} = 1 md
ϕ_f	= 0.00321
ϕ_{ma1}	= 0.00289
ϕ_{ma2}	= 0.318
h	= 545 ft
σ	= 4.94 10^{-6} ft^{-2}
Outer radius	= 6000 ft.
r_w	= 0.25 ft.
Flowrate	= 100 Stb/day

TABLE 3

SAMPLE CASE 3 RESERVOIR DESCRIPTION

Rock Compressibility	= 0.0005/psi
Over/under Burden Thickness	= 150 ft
Reservoir and Caprock Initial Temperature	= 75°F
Reservoir and Caprock Heat Capacity	= 35 BTU/cuft rock-°F
Reservoir and Caprock Thermal Conductivity	= 24 BTU/(ft-day-°F)
Block Dimensions X Direction	= 5,10,15,20,25,5,10,15,20,25 ft
Block Dimensions Y Direction	= 5 ft
Block Dimensions Z Direction	= 3 ft
Horizontal Permeabilities	= 50 md (cols 1-5) = 2000 md (cols 6-10)
Vertical Permeabilities	= Horizontal Permeabilities
Porosity	= 0.28 (cols 1-5) = 0.02 (cols 6-10)
Depth to Top of First Layer	= 1500 ft
Pressure at Datum Depth	= 150 psi
Datum Depth	= 1515 ft

TABLE 4

FRACTURE DOMAIN SATURATION FUNCTIONS

SW	KRW	KRH	PCW	SL	KRG	KROG	PCG
0.05	0	0.95	0	0.1	0.9	0	0
0.95	0.95	0	0	0.95	0	0.9	0

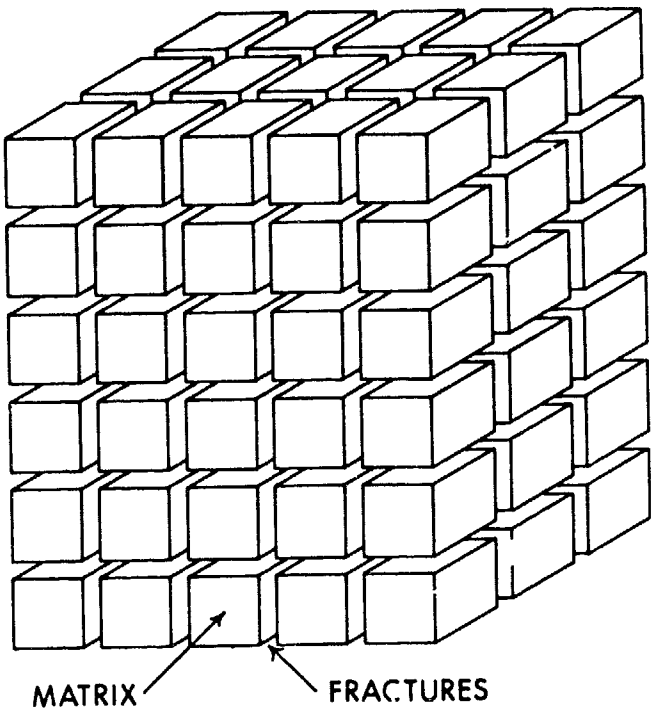

Fig. 1 – Idealized model of a naturally fractured reservoir

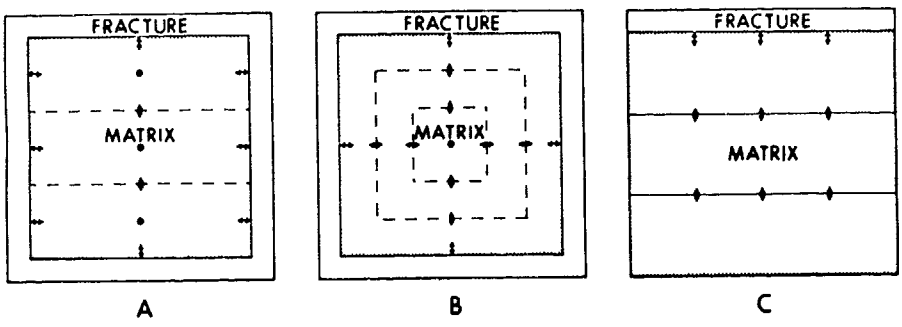

Fig. 2 – Dual porosity system with subdivision of matrix domain

TRIPLE POROSITY SYSTEM

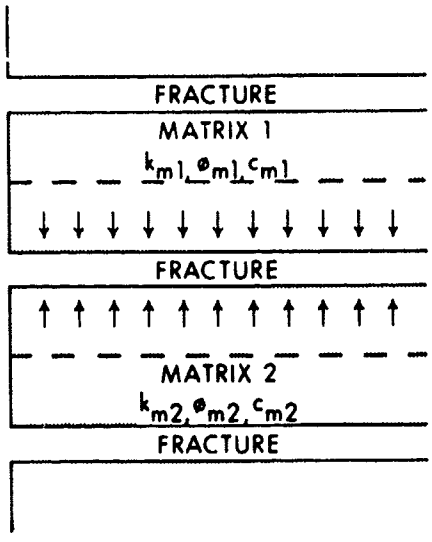

NO FLOW BETWEEN
MATRIX 1&2

Fig. 3 – Idealized triple porosity system

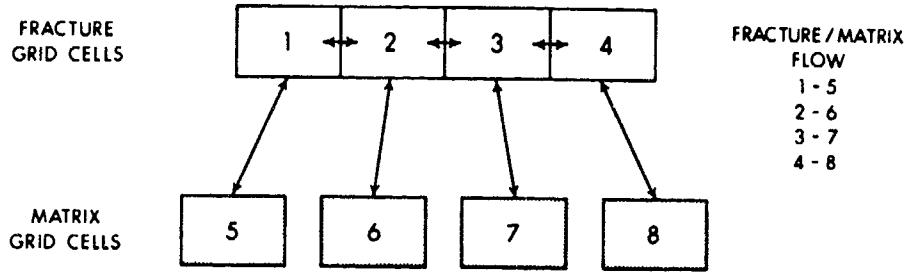

Fig 4—Simulation grid cells for a dual-porosity system

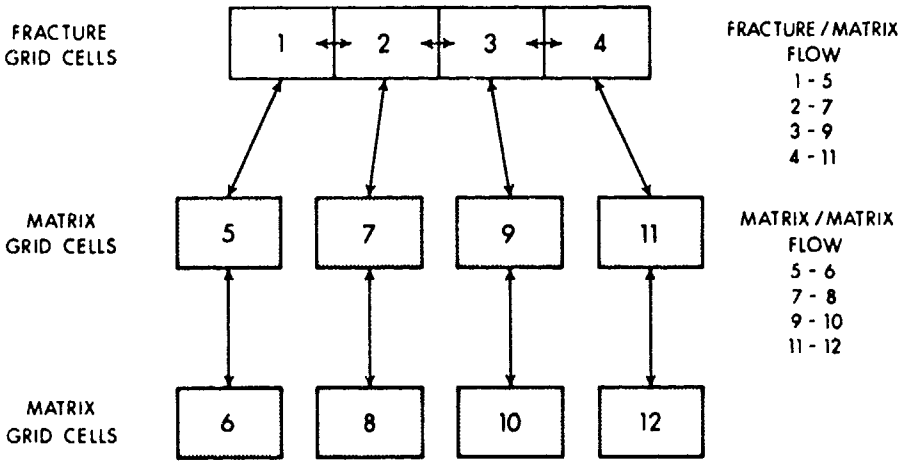

Fig 5—Simulation grid cells for a dual-porosity system with subdivision of matrix domain

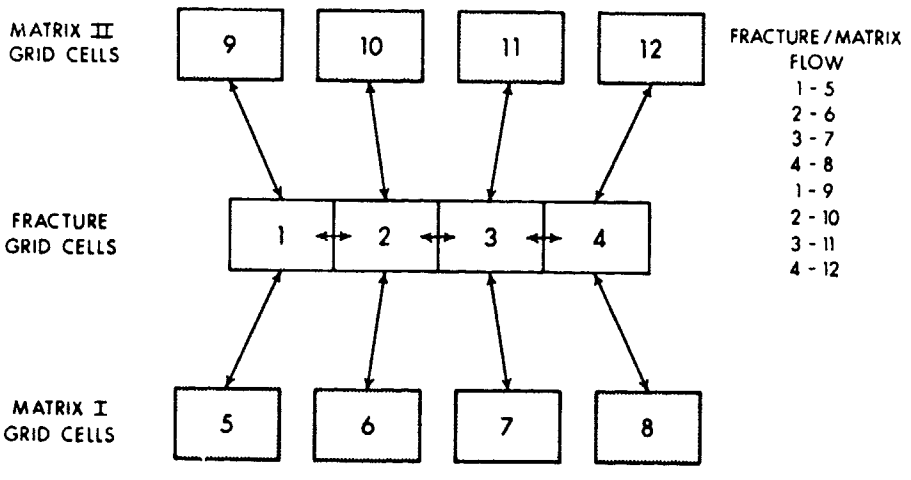

Fig 6—Simulation grid cells for a triple-porosity system

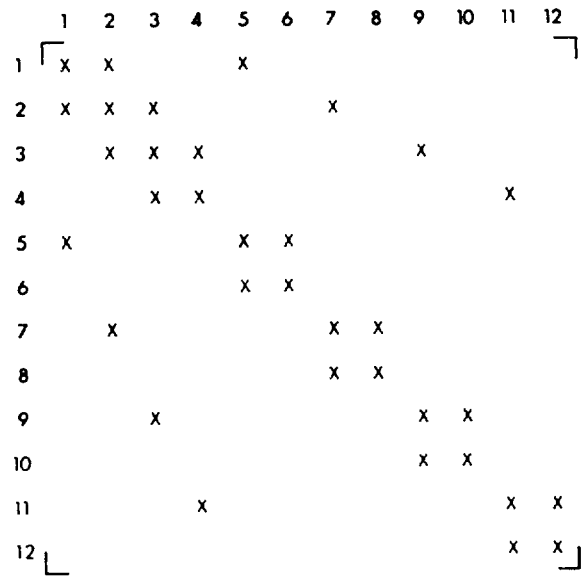

Fig 7—Matrix for Fig 5

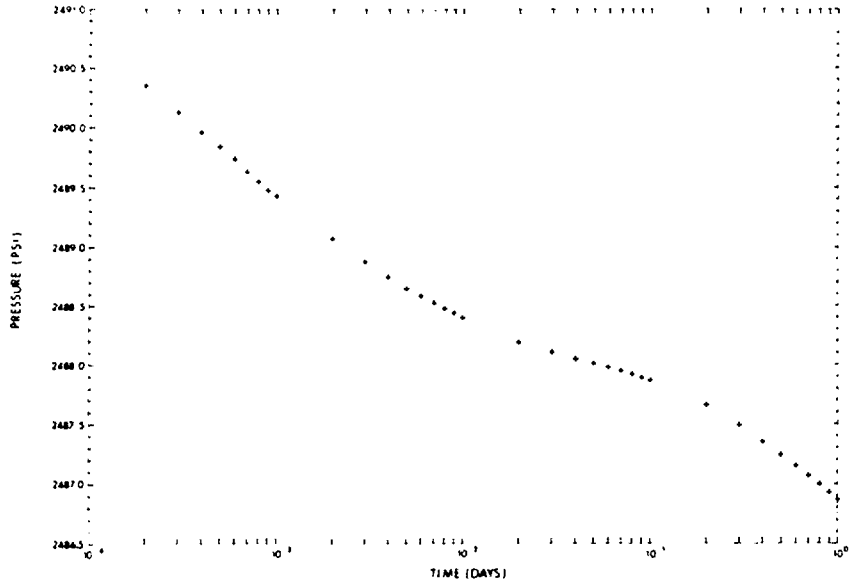

Fig 8—Sample Case 1—pressure drawdown behavior of a dual-porosity system

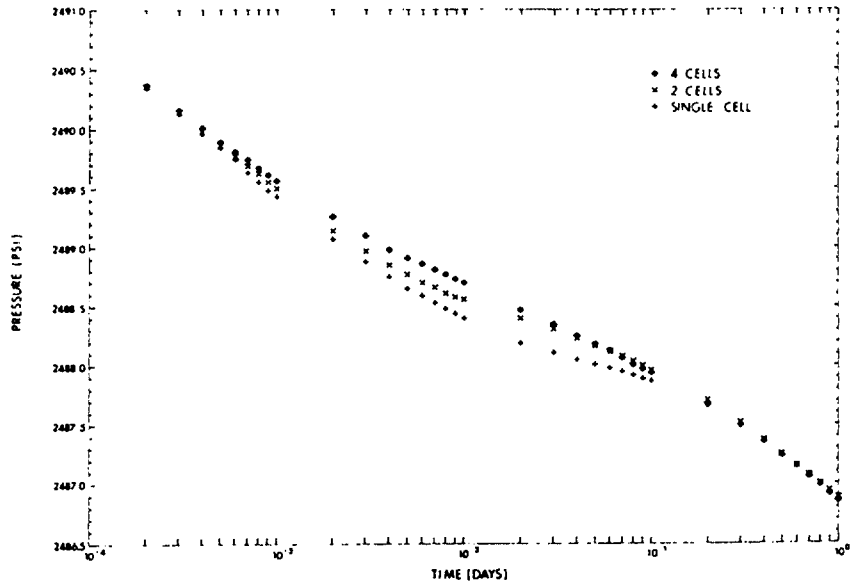

Fig 9—Sample Case 1—pressure drawdown behavior of a dual-porosity system with subdivision of matrix domain

SPE 16009

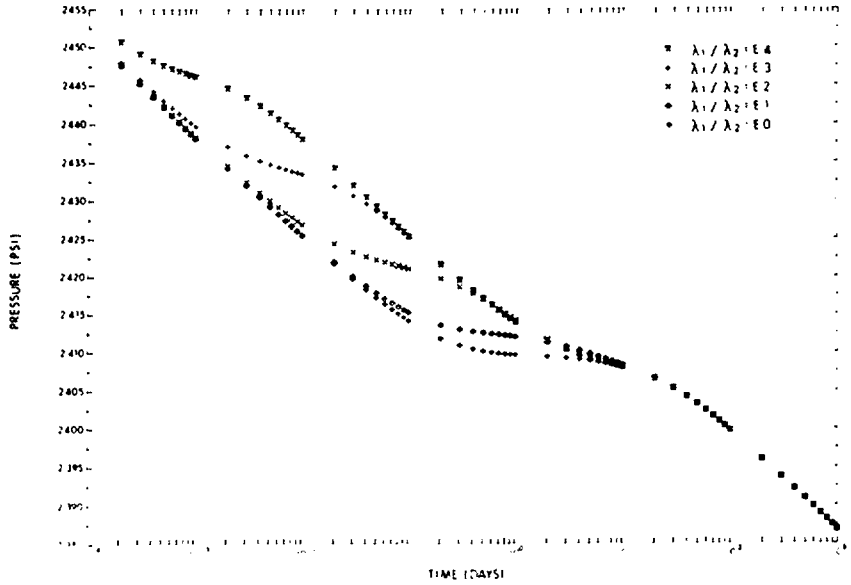

Fig. 10 - Sample Case 2 - pressure drawdown behavior of a triple-porosity system with

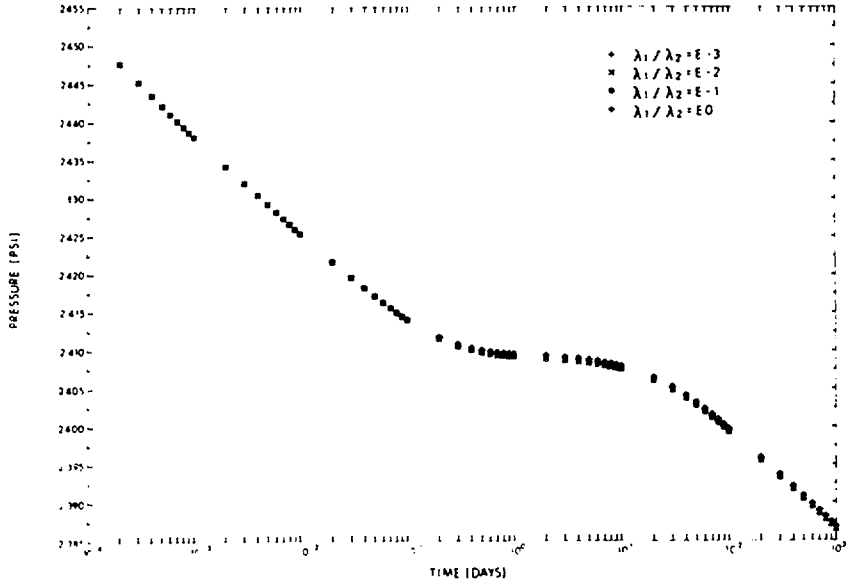

Fig. 11—Sample Case 2 – pressure drawdown behavior of a triple porosity system with

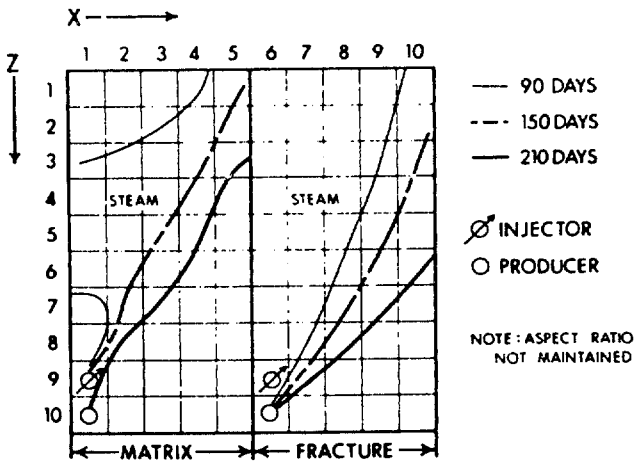

Fig. 12—Sample Case 3—growth of steam chamber

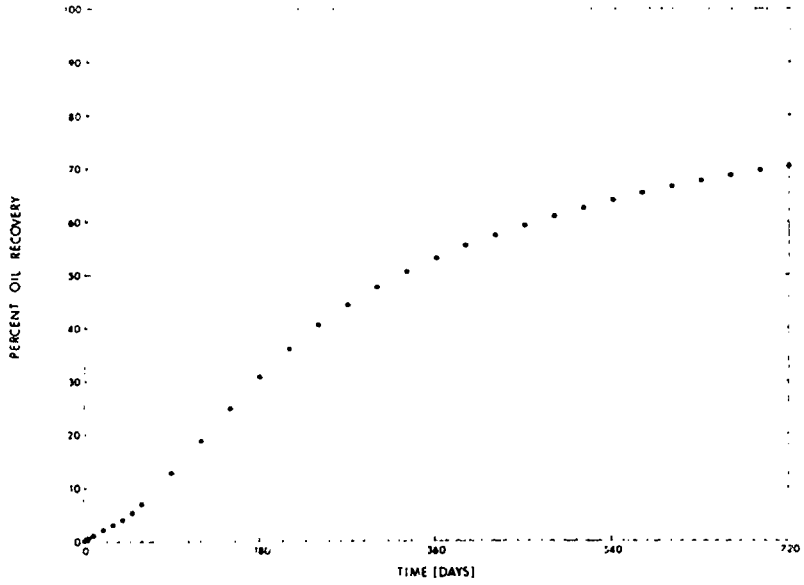

Fig. 13—Sample Case 3—oil recovery